Available online at www.sciencedirect.com
SCIENCE DIRECT
ELSEVIER
Polymer 46 (2005) 9022–9032
polymer
www.elsevier.com/locate/polymer

Shear amplification and re-crystallization of isotactic polypropylene from an oriented melt in presence of oriented clay platelets

Ke Wang, Yan Xiao, Bing Na, Hong Tan, Qin Zhang, Qiang Fu*

State Key laboratory of Polymer Materials Engineering, Department of Polymer Science and Materials, Sichuan University, Chengdu 610065, People's Republic of China

Received 10 March 2005; received in revised form 1 July 2005; accepted 7 July 2005
Available online 10 August 2005

Abstract

In this study, we first prepared isotactic Polypropylene (iPP)/organoclay nanocomposite specimens via twin-screw extruder and by adding compatibilizer (maleic anhybride grafted PP). Then PP and the composites were subjected to dynamic packing injection molding, in which the melt was firstly injected into the mold then forced to move repeatedly in a chamber by two pistons that moved reversibly with the same frequency as the solidification progressively occurred from the mold wall to the molding core part. The dispersion and orientation of layered organoclay in the nanocomposite were estimated by transmission electron microscopy (TEM) and 2d-wide angle X-ray scattering (2d-WAXS). A much higher degree of orientation of PP was found in the composites compared with the pure PP. This was explained by so called shear amplification in that a great enhancement of local stress occurred in the small interparticles region of two adjacent layered tactoids with different velocities. Furthermore, re-crystallization of isotactic polypropylene (iPP) by melting the dynamic packing injection molded samples has been investigated by polarizing light microscopy (PLM). A highly oriented threadlike crystallites was observed for the first time when crystallization occurs by melting the dynamic packing injection molded samples at 180 °C. However, spherulitic morphology is always obtained once PP crystallizes from an isotropic melt by melting the samples at 200 °C. The shear amplification mechanism and the formation mechanism of oriented threadlike crystallites have been discussed in detail.

Keywords: iPP/Organoclay nanocomposite; Shear amplification; Oriented threadlike crystallites

1. Introduction

Recently, polymer/layered silicate nanocomposites (PLSN) have gained intensive interest because of their unique and valuable mechanical [1,2], thermal [3], electronic [4,5] and permeability [6] properties compared to the pristine polymers; thereby numerous studies have been systematically carried out on the relationship between microstructure and meso-/macroscopic properties in PLSNs. Several semicrystalline polymers, such as polypropylene, polyamide and polyester, were usually selected as the basal resin of nanocomposite and the crystalline behaviors of these PLSNs played pivotal roles in determining the ultimate properties of as-prepared nanocomposites. Obviously, the incorporation of nanoscale-layered silicate into these semicrystalline polymers would dramatically impact the crystalline properties including crystallization kinetics, crystal structure and crystallinity. Two effects of nanoclay platelets are commonly considered on crystallization of basal polymers [7–10]: (i) Nanoclay layers is an effective heterogeneous nucleating agent for decreasing the interfacial free-energy per unit area perpendicular to macromolecular chains in PLS nanocomposites, which enhances the nucleating speed [11] and the crystallization rate [12,13], improves the cooling crystallization temperature [14] and decreases the spherulite size [9]; (ii) a physical hindrance of nanoclay layers to the motion of polymer chains limits the crystallization of basal polymer, resulting in a decrease of crystallinity [9] and degree of perfection of the crystal [8,15].

Besides these results noted above, silicate nanopaletlets could induce some other unique and unusual crystallization behaviors in PLSNs that are also valuable to summarize hereafter. Krikorian et al. [16] recently found that the

* Corresponding author. Tel.: +86 28 85460953; fax: +86 28 85405402.
E-mail address: qiangfu@scu.edu.cn (Q. Fu).

0032-3861/$ - see front matter © 2005 Elsevier Ltd. All rights reserved.
doi:10.1016/j.polymer.2005.07.025

nucleation rate was low but the spherulitic grow rate was high in poly(L-lactic acid) (PLLA)/organoclay nanocomposites with a high degree of exfoliated structure in contrasting to the system with a intercalated structure. However, the overall bulk crystallization rate was increased in the intercalated system but was retarded in the exfoliated system. Ghosh et al. [17] demonstrated that the clay dispersibility played a substantial role in altering the crystal structures in syndiotactic polystyrene(sPS)/layered clay nanocomposite: nanoscale dispersibility was found to promote rapid formation of α-form crystal; whereas pristine clay with aggregated structure was favorable for formation of β-form crystal, which was prevalent in pure sPS. Zhan et al. [19] also suggested that the addition of montmorillonite (MMT) promoted the transition of crystal structure from α-phase to β-phase crystal in polyamide 66/clay nanocomposite at various crystallization temperatures. The influence of crystallization on intercalation and morphology of PP/organoclay nanocomposite has been studied by Maiti et al. [20]. They found that the extent of intercalation of polymer chains into silicate galleries was increased with the increase of crystallization temperature due to a long time in molten state. A higher density of dispersed clay particles was observed in the inter-spherulitic region compared to the density inside-spherulite, which was presumably due to the segregation of the clay particles from the crystal growth front due to the exclusion. An unusual crystalline behavior in polyamide 6(PA6)/MMT nanocomposite was observed by Wu et al. [21] that increased cooling rate would result in higher crystallinity of PA6/MMT nanocomposite in sharp contrast to pure PA6 and other semicrystalline polymers. And the γ-form crystal was dominant in the rapidly cooling crystallization of nanocomposite. When the content of nanoclay was high, the confinement effect of physical hindrance of nanoclay platelets to the motion of polymer chains in crystal became stronger and even induced an 'abnormal' high temperature molten peak in DSC thermogram, which was reported by Phang [22] and Zhang [10] in polyester/clay and nylon 10,10/clay nanocomposites, respectively.

Early stage of shear-induced crystallization in PP/MMT nanocomposite has been investigated by Solomon [23] and Nowack [24]. For quiescent isothermal crystallization, the intercalated PP nanocomposite displayed retarded crystallization kinetics compared to that of pure PP; a flow-induced acceleration of crystallization kinetics was observed for PP nanocomposite whereas only a modest effect of shear strain on pure PP crystallization [23]. Nowack [24] recently suggested that only weak nucleating activity of nanoclay was inspected during crystallization in quiescent condition and the nucleation activity was greatly enhanced in shear-induced crystallization. Similarly, in the injection-molded specimen of nylon 6/clay nanocomposite, the nucleation density was significantly increased through orientation of macromolecules and the foreign particle effect of the nanoplatelets. Thus complete spherulitic formation was suppressed even in the core region of specimen at high mold temperature [25]. The levels of chains and crystals orientation in injection-molded nylon 6/clay nanocomposite were found obviously higher than that of pure nylon 6 sample by Cakmak et al. [34], and this was attributed to a so-called shear amplification mechanism that a great enhancement of local stress occurred in the small interparticles region of two adjacent layered tactoids with different velocities.

A typical 'shish-kebab' crystalline structure has been found by Maiti [26] and Kim [27] in polyamide/organoclay nanocomposite and by Choi [28] in PP/EPR/talc nanocomposite where a preferential orientation of polymer lamellae perpendicular to the surface of organoclaylayers was inspected by TEM measurements. The unique observation of lamellar orientation on the clay layers was ascribed to nucleation and epitaxial crystallization at the interface between layered silicate and polymer matrix especially the surfaces of clay platelets acted as heterogeneous nucleation sites. Moreover, a dramatic change in crystal morphology was observed in PP/clay nanocomposites when crystallization at high temperature, i.e. 142 °C, at which the pristine PP did not crystallize at all [29,30]. It was manifested that the crystallites exhibited fibrous structure that grew in length and diameter with time and even after a long prolonged crystallization time the crystalline morphology still remained threadlike shape. Moreover, at the beginning stage of crystallization in poly(ethylene terephthalate)/clay nanocomposite, some crystallites were fibrous [15]. The asymmetric morphology of crystal was also contributed to the surfaces of the partially exfoliated clay platelets acted as a nucleation agent, which promoted the crystallization of polymer.

In this article, we first prepared isotactic polypropylene (iPP)/organoclay nanocomposite specimens via twin-screw extruder and by adding compatibilizer (maleic anhybride grafted PP). Then PP and the composites were subjected to dynamic packing injection molding, in which the melt was firstly injected into the mold then forced to move repeatedly in a chamber by two pistons that moved reversibly with the same frequency as the solidification progressively occurs from the mold wall to the molding core part. In this way, the highly oriented structure for both iPP and clay layers can be obtained. Our proposals are mainly two folds: (1) Further explore the idea of shear amplification by checking the change of orientation along the sample thickness; (2) investigate the effect of oriented clay on the re-crystallization of iPP by melting the dynamic packing injection molded samples.

2. Experimental

2.1. Materials

A commercially available isotactic polypropylene (trade

marked as T30S, Yan Shan Petroleum China) with $M_\eta = 29.2\times10^3$ g/mol and a melt flow index (MFI) of 0.9975 g/min (190 °C, 2.16 kg) and a density of 0.91 g/m^3, was used as the basal polymer. The compatibilizer, PP grafted maleic anhybride (PP-MA) (MA content = 0.9 wt%, MFI = 6.74 g/min at 190 °C) in which maleic anhybride group is randomly grafted on a PP backbone, was purchased from Chen Guan Co. (Sichuan, China). Sodium montmorillonite with a cation exchange capacity (CEC) of 68.8 mmol/100 g (RenShou, Sichuan, China) was organically modified through ion-exchanged reaction with dioctadecyl dimethylammonium bromide and the detailed procedure can be found in our previous publication [31]. The thickness of organoclay tactoid comprised tens layers is in the range of 50–100 nm, while the length is about 300 nm. The diameter of clay particle aggregated by tactoids is less than 10 μm.

2.2. Preparation of PP/organoclay nanocomposites

A master-batch consisted of iPP/PP-MA/organoclay (80/20/20 wt%) was melt-mixed in a TSSJ-2S co-rotating twin-screw extruder. The temperature of the extruder was maintained at 160, 190, 210, 210 and 195 °C from hopper to die and the screw speed was about 110 rpm. Then a series iPP/PP-MA/organoclay nanocomposites with iPP/PP-MA/organoclay (90/10/x wt%, x = 0, 1, 3, 5, 10) were obtained through adding iPP and PP-MA to dilute the as-prepared master-batch in the extruder. Thereafter, the specimens are termed as PPCNx (where x represent the weight content of OMMT, such as PPCN3 means that the organoclay content is 3 wt%). After pelletized and dried, composites were injected into a mold with aid of a SZ 100 g injection-molding machine with barrel temperature of 190 °C and injection pressure of 900 kg cm^{-2}. Then dynamic packing injection molding (thereafter is abbreviated as DPIM) technology was applied. Its main feature was to introduce shear to the cooling melt during packing stage by two pistons that moved reversibly with the same frequency (1.0 Hz). Shear rate was about 10 s^{-1} calculated from the geometry of mold. The processing parameters and the characteristics and detail experiment procedure of DPIM were described in Refs. [32,33]. We also carried out injection molding under static packing by using the same processing parameters but without shearing for comparison purpose. The specimen obtained by dynamic packing injection molding is called dynamic sample, otherwise the specimen obtained by static packing injection molding is called static sample.

2.3. Characterizations

2.3.1. 2d-Wide-angle X-ray scattering (2D WAXS)

The two dimensional wide-angle X-ray scattering experiments (2D WAXS) were conducted using a Rigaku Denki RAD-B diffractometer. The wavelength of the monochromated X-ray from Cu Kα radiation was 0.154 nm and reflection mode was used. The samples were placed with the orientation (flow direction) perpendicular to the beams. The intensity was corrected by subtracting the background scattering. Azimuthal scan of 2D WAXS were made (040) plane of iPP at a step of 1° from 0 to 360°. The orientation of chains could be calculated by the orientation parameter f,

$$f = \frac{3\langle\cos^2\varphi\rangle - 1}{2} \tag{1}$$

$$\langle\cos^2\varphi\rangle = \frac{\int_0^{\pi/2} I(\phi)\sin\phi\cos^2\phi \mathrm{d}\phi}{\int_0^{\pi/2} I(\phi)\sin\phi \mathrm{d}\phi} \tag{2}$$

where ϕ is the angle between the normal of a given (hkl) crystal plane and shear flow direction, and I is the intensity. Its limiting values of orientation parameter f, taking $\phi = 0$ as the shear flow direction, are -0.5 for a perfect perpendicular orientation and $+1.0$ for a perfect parallel orientation. An un-oriented sample gives $f = 0$.

2.3.2. Transmission electron microscope (TEM)

The dispersion and orientation of organoclay layers in iPP matrix were inspected by transmission electron microscope (TEM). For TEM measurement, the ultra-thin sections ($\sim$100 nm) were cut in the direction parallel to the shear flow and the measurement was performed on a JEM-100 CX TEM instrument at an acceleration voltage of 80 kV.

2.3.3. Polarizing light microscopy (PLM)

The crystallization of iPP was investigated in situ by a Leica DMIP polarizing light microscopy (PLM) equipped with a Linkam THMS 600 hot stage under crossed polarizers. Thin slices were cut from the injection molded samples, inserted between two microscope cover-glasses, melted at 180 °C and squeezed to obtain thin films. Then, slices were held for 2 min at 180 °C to achieve thermal equilibrium. In subsequence, samples were cooled to room temperature at a constant rate of −3 °C/min. The course of non-isothermal crystallization was recorded by taking photomicrographs at appropriate intervals of time, using a Canon PowerShot 550 digital camera. The flow direction is horizontal in all PLM pictures of this study.

3. Results

3.1. Orientation of iPP and clay in the dynamic injection-molded sample

A structural hierarchy along thickness direction of injection molding specimens is manifested in Fig. 1,

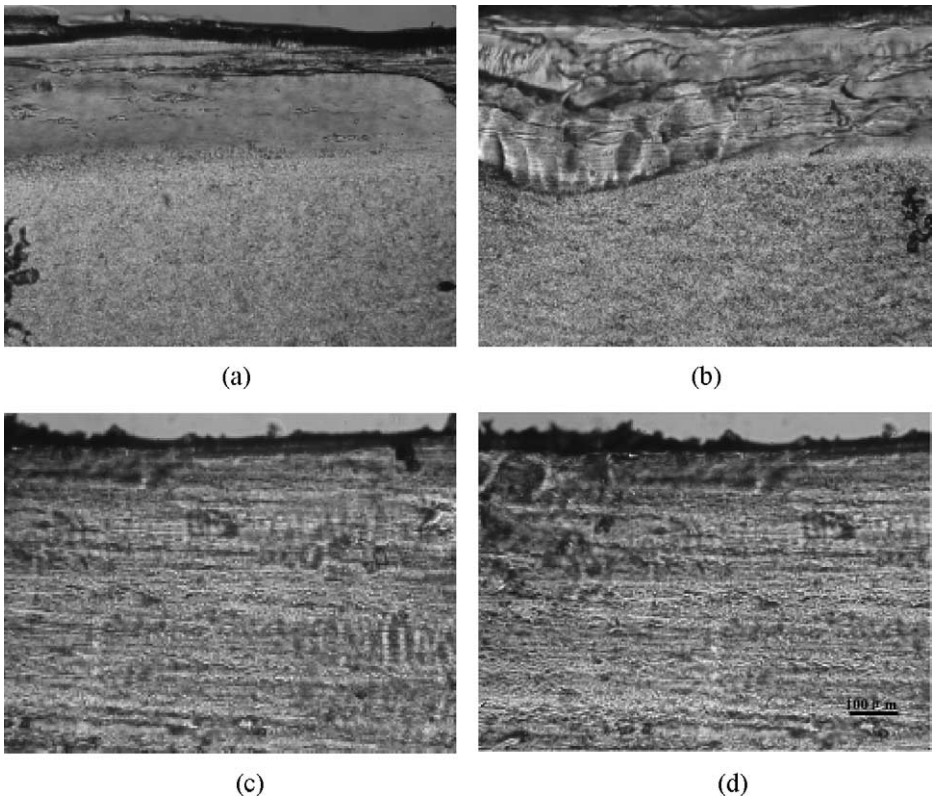

Fig. 1. PLM pictures represent the structural hierarchies in (a) static PPCN0, (b) static PPCN5, (c) dynamic PPCN0 and (d) dynamic PPCN5 specimens.

where the flow direction is horizontal. These PLM images are obtained before melting and can represent the original morphologies of as-prepared samples. As shown in Fig. 1(a) and (b), an oriented skin zone and an isotropic core zone is seen for static samples. The former was formed immediately after the melt was injected into the cold mold chamber and the high content of oriented texture induced by shear flowing can be preserved due to rapid cooling; whereas the melt in the internal part of mold cooled down slowly and the relaxation of oriented texture performed completely. There exists a distinct boundary between the skin zone and the core zone, so one can easily distinguish the skin from the core. The thickness of the skin is about 200 μm for static sample PPCN0 (Fig. 1(a)) and about 300 μm for static sample PPCN5 with 5 wt% OMMT dispersed in iPP matrix (Fig. 1(b)). A significant increase of skin thickness in PPCN5 compared to PPCN0 indicates that incorporation of organoclay into the polymer matrix promote the orientation content of injection molded specimen, which is consistent with the result obtained by Cakmak et al. [34] in polyamide/clay injection molded specimen. This can be explained by so called shear amplification in that a great enhancement of local stress occurred in the small interparticles region of two adjacent layered tactoids with different velocities. In contrast to the static samples, additional oriented texture is observed within inspection scope of PLM in the dynamic samples prepared through DPIM, as shown in Fig. 1(c) without OMMT and (d) with 5 wt% OMMT. In DPIM processing, the melt was forced to move reversibly during cooled solidification and a unique zone composed of oriented texture was formed between the skin and the core. Although the boundary between the skin and the oriented zone is ambiguous, one can take the zone located between 300 and 1100 μm as the oriented zone through comparison with the static samples.

If shear amplification does play a role for the enhanced orientation of iPP in presence of layered clay particles, one should see even greater effect for dynamic samples. For this reason we carried out 2d-WAXS measurements to get detailed orientation parameter for each sample, particularly for dynamic ones. As an instance, Fig. 2 shows the typical 2d-WAXS patterns of the skin, the oriented zone and the core in dynamic (a) PPCN0 and (b) PPCN10 samples, respectively. The 2d-WAXS patterns in Fig. 2 are the characteristic reflection of the α-form crystal of PP consisting of (110), (040), (130), (111) and (−131) reflections in sequence from the inner to the outer. The intensity of (*hk*0) reflection is significantly enhanced at the equatorial direction meaning that the iPP lamellae are preferentially aligned along the flow direction. Based on the 2d-WAXS measurements, the orientation order parameter is calculated to be −0.20, −0.15 and 0.0 in the skin, the oriented zone and the core for PPCN0, respectively. Though the skin and the oriented zone are oriented, still the core remains mostly un-oriented for dynamic sample PPCN0. As expected, much strong orientation is achieved in the skin

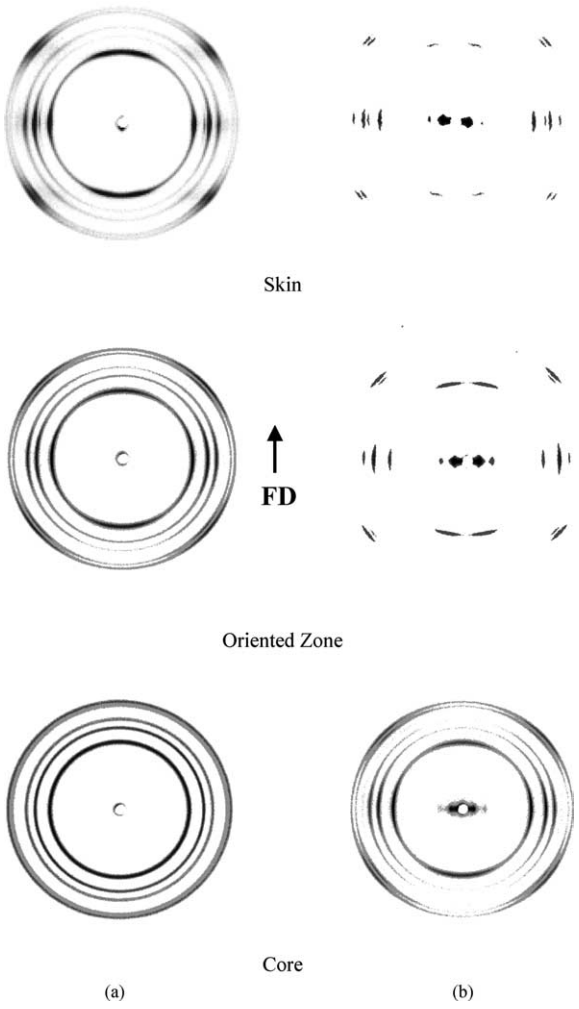

Fig. 2. Typical 2d-WAXS patterns represent the orientation levels of iPP molecular chains in (a) dynamic PPCN0 and (b) dynamic PPCN10 specimens. The flow direction is vertical.

and the oriented zones after the shear stress is applied during the processing. However, A dramatic increase of orientation even at the core is obtained for PP/clay nanocomposites. For example, the orientation order parameter becomes -0.26, -0.25 and -0.19 in the skin, the oriented zone and the core for PPCN10. The much higher orientation for the composites than that for pure iPP(PPCN0) indicates once again that there may indeed exist the shear amplification in iPP/clay nanocomposites. Meanwhile, the equatorial spots near the beam stopper in Fig. 2(b) are attributed to the periodic stack of organclay layers and imply that organoclay layers are also aligned parallel to the flow direction.

The orientation of clay layers along the shear flow direction was further proved by TEM observation. Fig. 3 shows the TEM results of (a) static sample PPCN5 at the core zone and (b) dynamic sample at the oriented zone, respectively. The dispersed OMMT is in nano-scale that the thickness of OMMT tactoids is less than 30 nm and numerous individual layers are detectable. The clay layers are seen much oriented along flow direction in the oriented zone but quite random in the core.

3.2. Constrained crystallization of iPP within oriented organoclay platelets

To see the effect of oriented clay platelets on the crystallization of iPP, melt re-crystallization by PLM was carried out by melting of dynamic samples at two different temperatures. One is 180 °C for 2 min to keep the oriented PP structure as much as possible. So one can investigates the crystal morphology of PP crystallization from an oriented melt within oriented clay platelets. The other is 200 °C for 5 min to destroy the oriented PP structure completely. In this way one could see the crystal shape of PP crystallization from an isotropic melt but within oriented clay platelets. Optical micrographs, taken during non-isothermal crystallization, cooling the skin zone of dynamic sample PPCN5 (together with PPCN0 for comparison) from 180 °C to room temperature, at a cooling rate of -3 °C/min, are shown in Fig. 4. A typical spherulitic growth is seen in PPCN0 sample that the nuclei appear at $\sim$132 °C and the diameters of spherulites gradually increase with the decrease of crystallization temperature (Fig. 4(a)). The spherulitic growth of PPCN0 indicates that the oriented structure obtained via dynamic packing injection molding can be easily destroyed and the crystallization occurs from an isotropic melt. However, an asymmetric fibrous crystalline growth in PPCN5 sample that numerous threadlike crystallites, whose length axes oriented parallel to flow direction, can be detected at $\sim$145 °C and then grow in length and diameter during cooling. Meanwhile, many tiny spherulites with small size are coexisting with the fibrils at low temperature in Fig. 4(b). Hambir [29] has elucidated the formation mechanism of fibrous crystal in PP/clay nanocomposite as the nucleating effect of surfaces of nanoclay layers to promote the crystallization of PP matrix. However, in our opinion, at least other two factors may contribute the fibrous crystal: (1) The high degree of orientation of PP achieved by the dynamic packing injection molding in the presence of clay (shear amplification as mentioned above), which can be preserved longer in the melting temperature and crystallization takes place from an oriented melt. (2) The confinement effect of nanoclay layers, which will restrict the relaxation of oriented PP chains, especially when the clay is oriented. It has been suggested by Medellin-Rodriguez et al. [35] that non-isothermal crystallization could be used to preserve the orientation of the clay induced by shear in nylon 6/clay nanocomposite. So we consider that the orientation of OMMT in the oriented zone of dynamic sample can be maintained in quiescent crystallization condition and which will play important role in the formation of fibrous crystals.

The confinement effect of the oriented nanoclay layers on PP crystallization can be further demonstrated by checking the loading effect of oriented OMMT. The PLM pictures

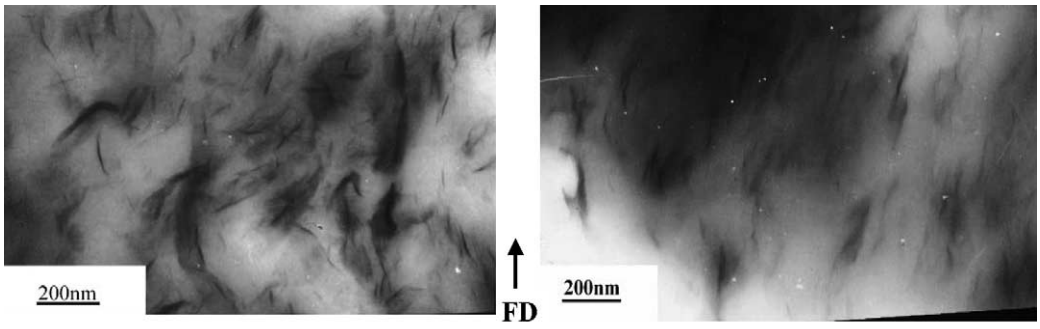

Fig. 3. TEM micrographs manifest the dispersion and orientation of layered OMMT in (a) the core zone of static PPCN5 and (b) the oriented zone of dynamic PPCN5 specimens.

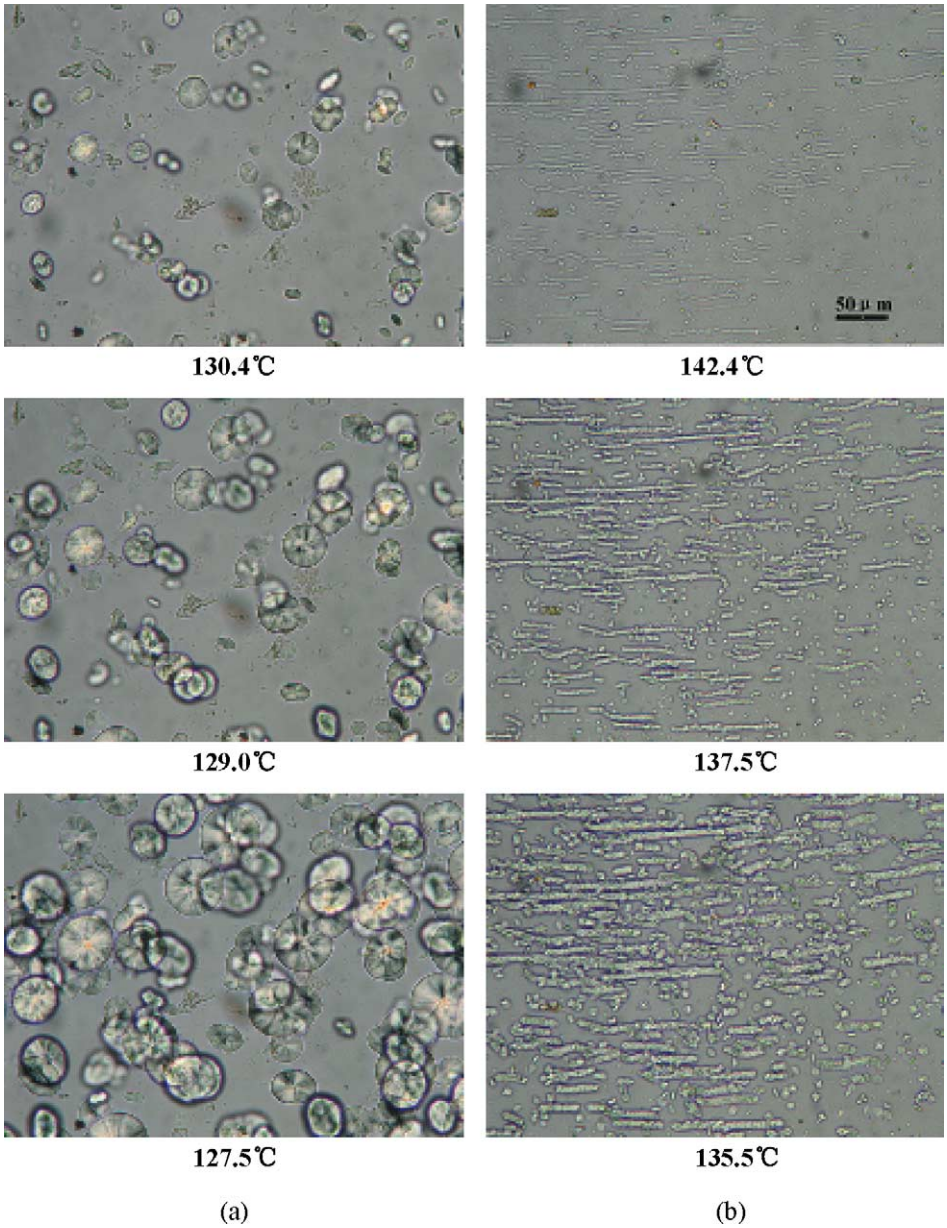

Fig. 4. PLM pictures show the sequences of crystal growth in the skin zones of (a) dynamic PPCN0 specimen and (b) dynamic PPCN5 specimen during non-isothermal crystallization.

marked with crystallization temperatures for PPCN1, PPCN3, PPCN5 and PPCN10 are presented in Fig. 5 and non-isothermal crystallization procedure is same as that of Fig. 4. When the content of OMMT is low (about 1 wt% in PPCN1), only spherulites are observed, as shown in Fig. 5(a). When the content of OMMT increases to 3 wt% in PPCN3, the fibrous crystals oriented parallel to the flow direction can be seen. The number density of oriented threadlike crystal is proportional to the content of OMMT loading from 3 to 10 wt%, which has been manifested in Fig. 5(b)–(d), especially Fig. 5(d) is mostly occupied by the fibrils as the OMMT content reached 10 wt%. As in situ observing the growth of fibrous crystal, the length of fibrous crystal no longer increased after certain growth stage and only increase in diameter was observed, and an example is given in Fig. 6. The L as indicated in Fig. 6 is taken as the final length of the fibrous crystal marked by red circle. So the average length of fibrous crystals can be calculated from the as-received PLM images. The average length of fibrous crystals is about 40, 70 and 110 μm in PPCN3, PPCN5 and PPCN10, respectively. And these length values are obtained as the average of at least 30 data. Since the degree of orientation is not much different among these samples, the increased length of fibrous crystal as increasing of clay content suggests an enhanced confinement at higher clay content. It should be noted that the fibrous crystal has been frequently reported in literatures, but to our knowledge, the highly oriented threadlike crystallites of PP is observed b y us for the first time.

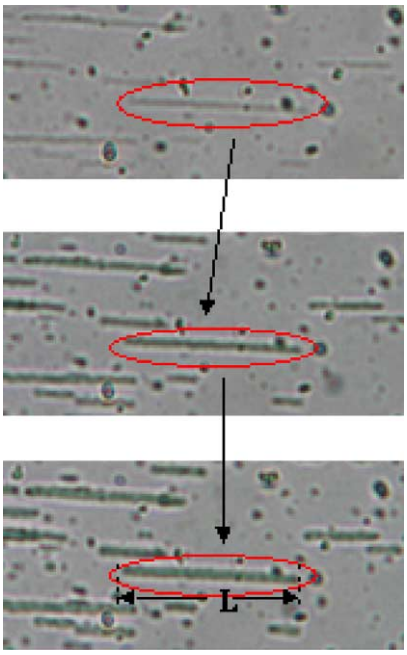

Fig. 6. An example shows how to calculated the maximum length of fibrous crystal.

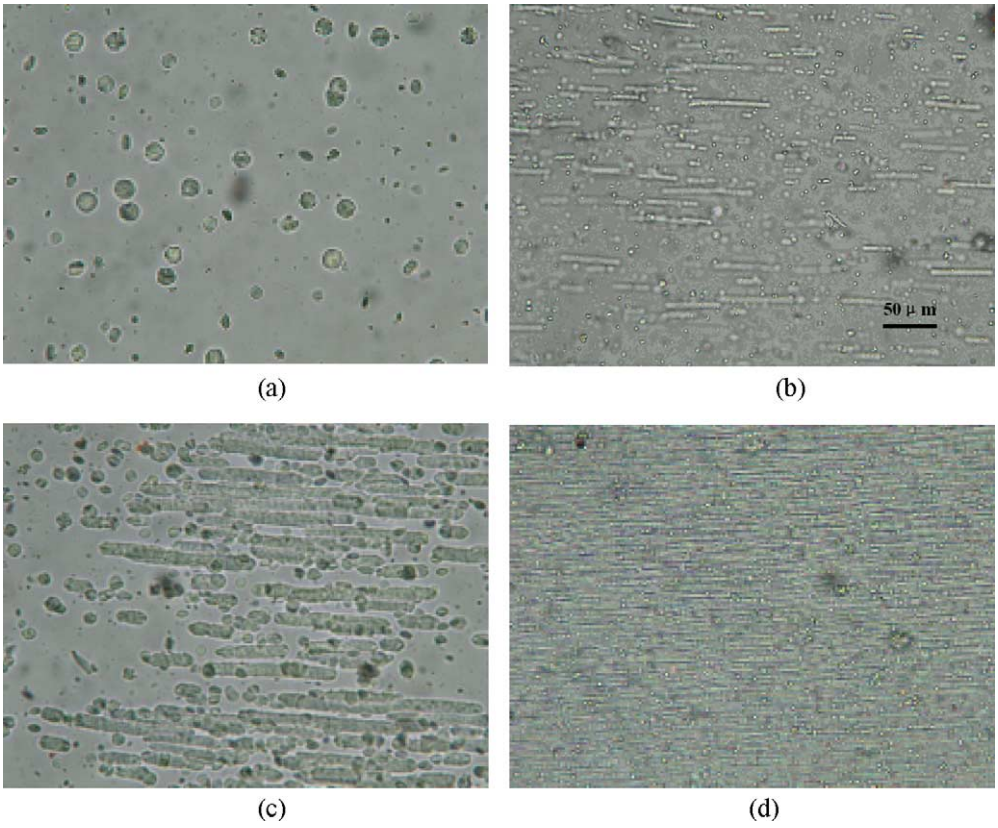

Fig. 5. PLM pictures represent the effect of OMMT content on the crystal morphologies in the oriented zones of (a) PPCN1 (taken at 133.8 °C), (b) PPCN3 (taken at 139.0 °C), (c) PPCN5 (taken at 134.8 °C) and (d) PPCN10 (taken at 146.3 °C).

When the oriented nanocompsoite samples are melted at a higher temperature, i.e. 200 °C, the growth type of crystal is significantly different to Fig. 5 and only spherulites develop irrespective to the content of organoclay. As displayed in Fig. 7, after the oriented zones of dynamic PPCN3, PPCN5, PPCN10 samples was heated to 200 °C, one observes always spherulitic morphology, no oriented threadlike crystallites anymore, even in this case the clay layers may still keep in oriented state. This result indicates that the oriented structure of PP can be destroyed at a higher temperature and crystallization occurs from an isotropic melt. In other words, once PP crystallizes from an isotropic melt, spherulites morphology are obtained, no matter the presence of clay and no matter the clay layers are oriented or not. Comparing the crystal morphology from an oriented zone of a dynamic sample and from the core of a static sample can further prove this argument. The TEM result above has shown a highly oriented clay layers in the oriented zone but random distribution of clay layers in the core. Fig. 8 shows the crystal morphology of PPCN5 crystallized from the oriented zone of the dynamic sample and the core of the static sample, respectively (non-isothermal crystallization procedure is same as that of Fig. 4). Again one observes a spherulitic growth in the core of static sample with disordered dispersion of organoclay (Fig. 8(a)) and an asymmetric fibrous crystalline growth in the oriented zone of dynamic sample with high oriented degree of organoclay (Fig. 8(b)). Meanwhile, the fibrils also orderly align with their length axes are parallel to the flow direction.

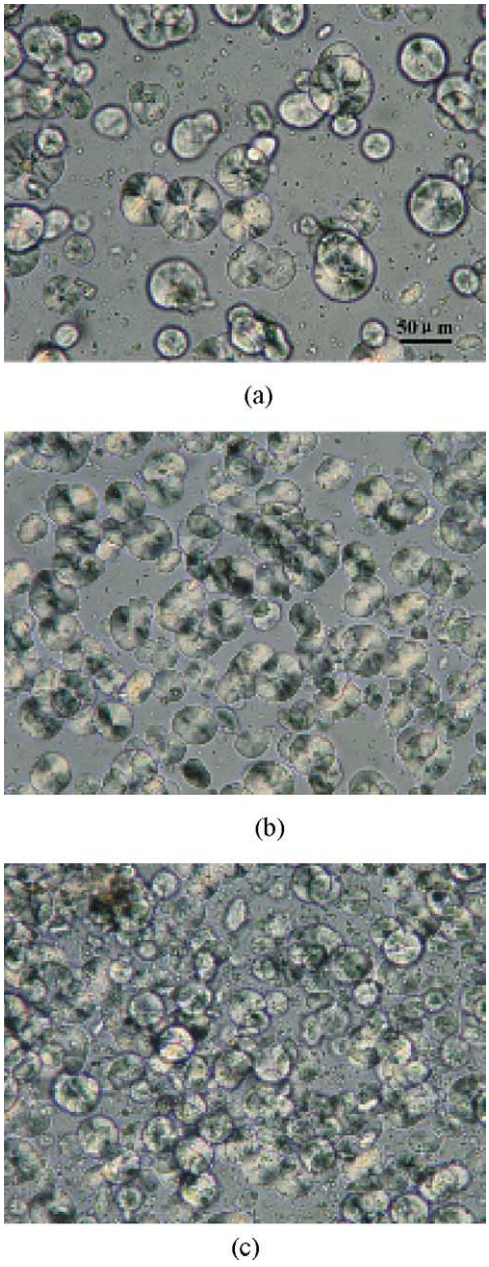

Fig. 7. PLM pictures show the crystal morphologies in the oriented zones of (a) PPCN3 (taken at 127.1 °C), (b) PPCN5 (taken at 1128.3 °C) and (c) PPCN10 (taken at 128.8 °C) after the samples were melted at a higher temperature (200 °C) for 5 min.

4. Discussion

4.1. Shear amplification

Shear amplification is very interesting and important concept that was proposed first by Cakmak et al. [34] to explain the enhanced orientation of injection molded nylon 6/clay nanocomposite. The detailed mechanism of shear amplification has been elucidated by Cakmak, where a great enhancement of local stress is suggested in the small interparticles region of two adjacent layered tactoids with different velocities. If the concept is really established, it will provide us a new way to achieve highly oriented structure in injection molded products by just introducing of layered platelets (not necessary clay). Here in our work, we purposely introduce the shear force during the packing stage, and have observed even more obvious enhanced orientation of PP molecules in presence of clay platelets. Usually, the achieved degree of orientation depends on the molecular chain orientation under external force and relaxation of the oriented chain. The growth of oriented PP molecular chains is mainly dependent of shear rate encountered during dynamic packing injection molding. Since the shear stress, τ, keeps unchanged, shear rate is related to the viscosity, η, expressed by $\dot{\gamma} = \tau/\eta$. It is clear that shear rate is inverse proportional to the viscosity. The viscosity of pure PP and the composites has been measured by using a Rheometric Scientific ARES rheometer with 25 mm diameter parallel plates at 190 °C over a shear rate range, $\dot{\gamma}$, from 10^{-1} to 10^{2} s^{-1} (the shear rate during DPIM processing is within this range), and is presented in Fig. 9. It is obvious that the viscosity of PP increases greatly by adding clay in whole range, particularly at the low shear rate range. One expects a reduced orientation of PP by adding clay if the processing condition keeps constant because $\dot{\gamma}$

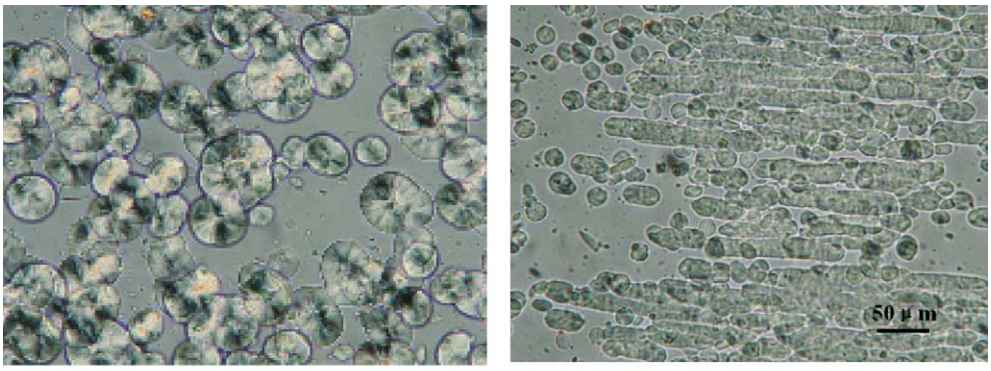

Fig. 8. PLM pictures represent the forms of crystal growth corresponded to (a) the core zone of static PPCN5 and (b) the oriented zone of dynamic PPCN5, respectively (the picture (a) is taken at 126.9 °C and (b) is taken at 132.8 °C).

decrease as increasing of viscosity. Thus the enhanced orientation observed could be only explained by shear amplification. The restriction of clay platelets on the relaxation of oriented PP chain, may also contributes to the enhanced orientation of PP, but certainly less important. Shown as an example, Fig. 10 is the heating curves of PPCN0, PPCN1 and PPCN5 after isothermal crystallization at 135 °C. It can be seen that melt point of PPCN5 is lower than that of PPCN0 by about 3 °C. If the molecular motion is retarded by confined environment during crystallization, the crystal growth will be hindered, resulting in a low regularity of spherulite and a small size of crystal. So the decrease of Tm can be expected.

4.2. The formation mechanism of oriented threadlike crystallites

It can be deduced from the previous literatures [36–38] that the addition of nanoclay platelets is not always necessary for the formation of asymmetric fibrous crystals. In those systems, the anisotropic crystal structure was due to crystallization of oriented iPP chains induced by shearing. As for our oriented iPP/OMMT nanocomposites, the formation mechanism of preferentially oriented fibrous crystal, which is corresponded well with the observations of PLM measurements, is discussed as follow.

For distinguishing the roles of oriented clay on the formation of the oriented asymmetric crystal growth, the influences of orientation and content of highly anisotropic organoclay should be considered. The orientation of layered organoclay obviously affects the type of crystal growth that preferentially oriented fibrous crystals develop in the oriented zone of dynamic sample. While only conventional spherulites can be seen in the isotropic core zone of static sample, in which layered organocaly is randomly dispersed in the iPP matrix. Nevertheless, the crystal grows as spherulite in the oriented zone of dynamic PPCN1 sample with low content of organoclay (1 wt%) and the fibrils are observed at higher content of organocaly ($\geq$3 wt%), which means that a critical required content should be satisfied to ensure the formation of the oriented fibrous crystal. Meanwhile, the number density and average length of fibrous crystal are proportional to the increase of OMMT

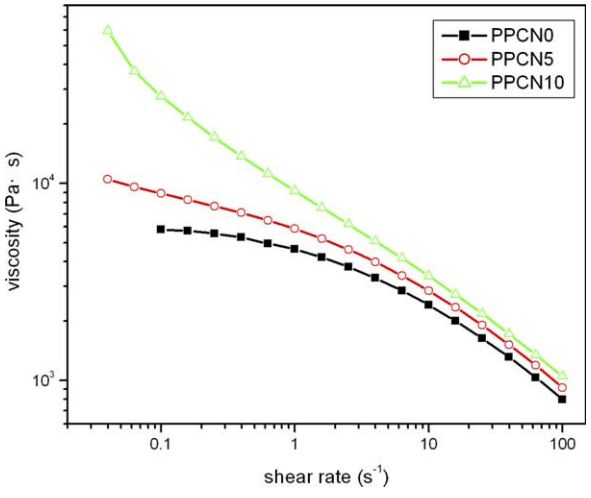

Fig. 9. Rheological curves represent the relationship of melt viscosity vs. shear rate in the pure PP and the composites.

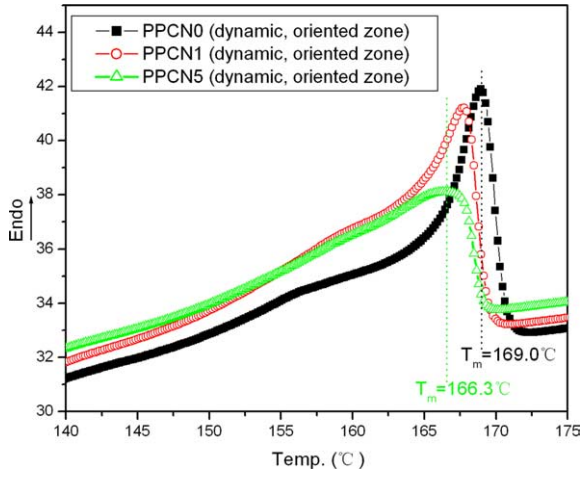

Fig. 10. DSC heating curves of as-prepared injection-molded specimens.

content that further manifested the importance of organocaly content on the growth of fibrous crystal. If the formation mechanism is ascribed to the effect of nucleation of nanoclay surface, the growth of threadlike crystal should be independent to the oriented state and loading of nanodispersed organoclay. Otherwise, the threadlike crystals should be mainly from a constrained crystal growth. The relaxation/motion of oriented iPP chain is restricted by its neighboring confinement environment exerted by preferentially oriented alignment of organoclay tactoids/platelets. Thus crystallization occurs from an oriented melt within oriented clay platelets. The crystal is forced to grow between the oriented clay platelets during non-isothermal crystallization, whereas the nucleation effect of nanodispersed silicate layers is less important in such processing. A sketch representing the crystallization of oriented iPP chains within confinement geometry constructed by preferentially oriented OMMT tactoids/platelets is shown in Fig. 11(b), and the free relaxation of extended chains in melt is also described in Fig. 11(a) for comparison purpose.

5. Conclusion

In summary, a highly oriented structure with both PP chain and clay platelets oriented along the shear flow direction has been obtained via dynamic packing injection molding. A much higher degree of orientation of PP was found in the composites compared with the pure PP. This was explained by so called shear amplification in that a great enhancement of local stress occurred in the small interparticles region of two adjacent layered tactoids with different velocities. The concept is very interesting and important. It is worth to be further investigated. Once it is established, will provide us a new way to achieve highly oriented structure in injection-molded products by just introducing of layered platelets. Furthermore, A highly oriented threadlike crystallites was observed for the first time when re-crystallization occurs by melting the dynamic packing injection molded samples at 180 °C. However, spherulitic morphology is always obtained once PP crystallizes from an isotropic melt by melting the samples at 200 °C. The threadlike crystals may be mainly from a constrained crystallization, where the relaxation/motion of oriented iPP chain is restricted by its neighboring confinement environment exerted by preferentially oriented alignment of clay tactoids/platelets. The crystal is forced to grow between the oriented clay platelets during crystallization.

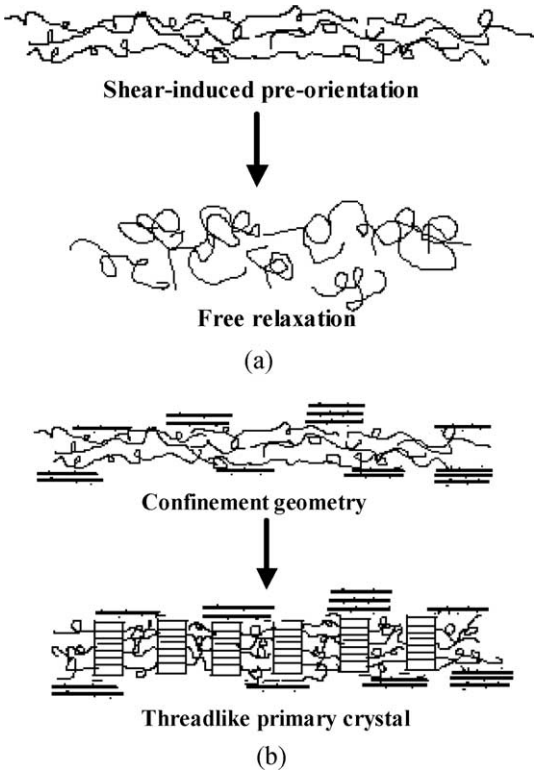

Fig. 11. Schematic representations of (a) free relaxation of extended chains in melt equilibrium process induced conventional spherulitic growth and (b) crystallization of oriented iPP chains within confinement geometry constructed by preferentially oriented OMMT tactoids/platelets resulted in threadlike crystal growth.

Acknowledgements

We would like to express our sincere thanks to National Natural Science Foundation of China (20490220, 20404008) for Financial Support. This work was subsidized by the Special Funds for Major State Basic Research Projects of China (2003CB615600). This work is also partly supported by Ministry of Education as a key project (104154).

References

[1] Dai XH, Xu J, Guo XL, Lu Y, Shen D, Zhao N, et al. Macromolecules 2004;37:5615.
[2] Liu XH, Wu QJ. Polymer 2001;42:10013.
[3] (a) Giannelis EP. Appl Organoment Chem 1998;12:675.
(b) Jimenez G, Ogata N, Kawai H, Ogihara T. J Polym Sci, Part B: Polym Sci 1997;2211.
[4] Hwang JJ, Liu HJ. Macromolecules 2002;35:7314.
[5] Nascimento GM, Constantino VRL, Temperini MLA. Macromolecules 2002;35:7535.
[6] (a) Bharadwaj PK. Macromolecules 2001;34:337.
(b) Osman MA, Mittal V, Lusti HR. Macromol Rapid Commun 2004; 25:1145.
[7] Lu YL, Zhang Y, Zhang GB, Yang MS, Yan SK, Shen DY. Polymer 2004;45:8999.
[8] Maio ED, Iannace S, Sorrentino L, Nicolais L. Polymer 2004;45: 8893.
[9] Ma J, Zhang SM, Qi ZN, Li G, Hu YL. J Appl Polym Sci 2002;83: 1978.
[10] Zhang GS, Yan DY. J Appl Polym Sci 2003;88:2181.
[11] Zhang X, Yang M, Zhao Y, Zhang SM, Dong X, Liu X, et al. J Appl Polym Sci 2004;92:552.

[12] Nam JY, Ray SS, Okamoto M. Macromolecules 2003;36:7126.
[13] He JD, Cheung MK, Yang MS, Qi ZN. J Appl Polym Sci 2003;89:3404.
[14] Zhang QX, Yu Z, Yang MS, Ma J, Mai YW. J Polym Sci, Part B: Polym Sci 2003;41:2861.
[15] Wan T, Chen L, Chua YC, Lu XH. J Appl Polym Sci 2004;94:1381.
[16] Krikorian V, Pochan DJ. Macromolecules 2004;37:6480.
[17] Ghosh AK, Woo EM. Polymer 2004;45:4749.
[19] Zhan ZD, Yu WX, Liu YH, Zhang JQ, Shao ZJ. Mater Lett 2004;58:802.
[20] Maiti P, Nam PH, Okamoto M, Hasegawa N, Usuki A. Macromolecules 2002;35:2393.
[21] Wu QJ, Liu XH, Berglund LA. Macromol Rapid Commun 2001;22:1438.
[22] Phang IY, Pramoda KP, Liu T, He CB. Polym Int 2004;53:1282.
[23] Somwangthanaroj A, Lee EC, Solomon MJ. Macromolecules 2003;36:2333.
[24] Nowacki R, Monasse B, Piorkowska E, Galeski A, Haudin JM. Polymer 2004;45:4877.
[25] Yalcin B, Cakmak M. Polymer 2004;45:2691.
[26] Maiti P, Okamoto M. Macromol Mater Eng 2003;288:440.
[27] Kim GM, Lee DH, Hoffmann B, Kressler J, Stoppelmann G. Polymer 2001;42:1095.
[28] Choi WJ, Kim SC. Polymer 2004;45:2393.
[29] Hambir S, Bulakh N, Kodgire P, Kalgaonkar R, Jog JP. J Polym Sci, Part B: Polym Sci 2001;29:446.
[30] Hambir S, Bulakh N, Jog JP. Polym Eng Sci 2002;42:1800.
[31] Zhang Q, Wang K, Men Y, Fu Q. Chin J Polym Sci 2003;21:359.
[32] (a) Guan Q, Shen KZ, Li J, Zhu J. J Appl Polym Sci 1995;55:1797.
(b) Zhang G, Jiang L, Shen KZ, Guan Q. J Appl Polym Sci 1999;71:799.
[33] Zhang Q, Wang Y, Fu Q. J Polym Sci, Part B: Polym Sci 2003;41:1.
[34] Yalcin B, Valladares D, Cakmak M. Polymer 2003;44:6913.
[35] Medellin-Rodriguez FJ, Burger C, Hsiao BS, Chu B, Vaia R, Phillips S. Polymer 2001;42:9015.
[36] Huo H, Jiang SC, An LJ, Feng JC. Macromolecules 2004;37:2478.
[37] Elmoumni A, Winter H, Waddon AJ, Fruitwala H. Macromolecules 2003;36:6453.
[38] Seki M, Thurman DW, Oberhauser JP, Kornfield JA. Macromolecules 2002;35:2583.